

# Kernel Methods in the Deep Ritz framework: Theory and practice

Hendrik Kleikamp \*      Tizian Wenzel<sup>†</sup>

October 7, 2024

## Abstract

In this contribution, kernel approximations are applied as ansatz functions within the Deep Ritz method. This allows to approximate weak solutions of elliptic partial differential equations with weak enforcement of boundary conditions using Nitsche’s method. A priori error estimates are proven in different norms leveraging both standard results for weak solutions of elliptic equations and well-established convergence results for kernel methods. This availability of a priori error estimates renders the method useful for practical purposes. The procedure is described in detail, meanwhile providing practical hints and implementation details. By means of numerical examples, the performance of the proposed approach is evaluated numerically and the results agree with the theoretical findings.

**Keywords:** Deep Ritz method, kernel methods, energy minimization, partial differential equations, Nitsche’s method, a priori error estimation

**MSC Classification:** 46E22, 65N30, 68T01

## 1 Introduction

Application of different machine learning tools to approximate solutions to partial differential equations (PDEs) has been an active direction of research in the past years [27, 4]. A particularly prominent example is the *deep Ritz method*, first introduced in [8], which makes use of the equivalent formulation of a variational problem as an energy minimization task. In the original deep Ritz method, deep neural networks are used as ansatz functions.

In this contribution, we replace the neural networks in the deep Ritz method by kernel methods (see Section 2.2 for a short introduction into kernel methods). The linear structure of the resulting ansatz space allows for simple yet powerful a priori error estimates and convergence rates. Such error estimates and convergence rates are only rarely available for neural networks in the deep Ritz context and require extensive analysis, see [18, 12].

Meshless methods gained attention in the past decades to solve several different types of PDEs, see for instance [26] and [2] for review articles on this topic. Compared to classical mesh-based methods such as the finite element method, meshless methods do not require the (potentially complex and costly) meshing of the underlying computational domain. In the context of kernel approximations and radial basis functions, there are various methods such as symmetric kernel collocation [11], Kansa method [13] or radial basis function finite differences [10]. Here we are concerned with the kernel Galerkin approach introduced in [33], which uses kernels as ansatz functions in the Galerkin method to solve variational formulations of elliptic PDEs. This approach was further developed and used for instance to solve elliptic

---

\*Institute for Analysis and Numerics, Mathematics Münster, University of Münster, Einsteinstrasse 62, 48149 Münster, Germany, ([hendrik.kleikamp@uni-muenster.de](mailto:hendrik.kleikamp@uni-muenster.de)), funded by the Deutsche Forschungsgemeinschaft (DFG, German Research Foundation) under Germany’s Excellence Strategy EXC 2044 –390685587, Mathematics Münster: Dynamics–Geometry–Structure.

<sup>†</sup>Department of Mathematics, Universität Hamburg, Bundesstraße 55, 20146 Hamburg, Germany, ([tizian.wenzel@uni-hamburg.de](mailto:tizian.wenzel@uni-hamburg.de)), acknowledgement of financial support through the projects LD-SODA of the *Landesforschungsförderung Hamburg* (LFF) and support from the RTG 2583 “Modeling, Simulation and Optimization of Fluid Dynamic Applications” funded by the *Deutsche Forschungsgemeinschaft* (DFG).

and parabolic PDEs on spheres in [23, 17] or to define an energy conservative scheme for nonlinear wave equations in [30]. However, it turns out that already for elliptic equations, the resulting stiffness matrices suffer from large condition numbers, see for instance [7], and are costly to compute due to the required global numerical integration for every pair of ansatz functions. The approach described in this contribution constitutes a possible alternative to deal with these difficulties. Furthermore, the error estimates derived in [33] still hold for our method. We additionally improve the theoretical statements by taking into account the most recent results on approximation errors for kernel methods.

As an additional difference to the energy minimization problem formulated in [8], we consider a weak formulation that is consistent with the strong formulation. To this end, we apply Nitsche's method [24] and still impose the Dirichlet boundary conditions in a weak manner. In order to confirm the convergence rates predicted by the theory, the consistency of our formulation enables a comparison to the strong solution in the numerical examples considered in Section 4.

The paper is organized as follows: In Section 2, we provide the theoretical background on weak formulations of PDEs required for the deep Ritz method. We additionally recall some basic statements from numerical analysis of Galerkin methods that will be used later to prove a priori estimates in different norms. Furthermore, we give details on kernel methods and state well-known approximation error estimates for these approaches in Sobolev norms. Afterwards, in Section 3, the details regarding a conjunction of the deep Ritz method and kernel approximation are provided. In Section 3.2, an a priori error estimate for the approach introduced in detail in Section 3.1 is proven based on the theoretical foundations from Section 2. Furthermore, some practical aspects are considered in Section 3.3. Before finishing the paper with an outlook and a conclusion in Section 5, we show and discuss several numerical experiments in Section 4 that confirm the theoretical results given before and highlight the potential of the proposed methodology.

## 2 Theoretical background

Before discussing the application of kernel methods in the deep Ritz approach, we will first review key definitions and notations related to the variational formulation of elliptic PDEs and the Dirichlet principle, followed by an introduction to kernel methods.

### 2.1 Variational formulation for elliptic PDEs and energy minimization

Let  $\Omega \subset \mathbb{R}^d$  for some  $d \in \mathbb{N}$  be a bounded domain. We denote by  $\Gamma_D \subset \partial\Omega$  the Dirichlet boundary part of  $\Omega$  and by  $\Gamma_N \subset \partial\Omega$  the Neumann boundary part. We assume that it holds  $\Gamma_D \cup \Gamma_N = \partial\Omega$  and  $\Gamma_D \cap \Gamma_N = \emptyset$  and that  $\Gamma_D$  and  $\Gamma_N$  are Lipschitz continuous. Further, let  $\kappa \in L^\infty(\Omega; \mathbb{R}^{d \times d})$  such that  $\kappa$  is symmetric almost everywhere and in addition elliptic, i.e. there exists a constant  $\alpha > 0$  such that

$$\langle \kappa(x)\xi, \xi \rangle \geq \alpha \|\xi\|^2 \quad \text{for all } \xi \in \mathbb{R}^d \text{ and almost all } x \in \Omega.$$

Let  $f \in L^2(\Omega)$ ,  $g_D \in H^{1/2}(\Gamma_D)$ ,  $g_N \in H^{1/2}(\Gamma_N)$  and  $\rho \in L^\infty(\Omega)$  such that  $\rho \geq 0$  almost everywhere. We consider as an example the weak formulation of the following diffusion problem

$$\begin{aligned} -\nabla \cdot (\kappa \nabla u) + \rho u &= f & \text{in } \Omega, \\ u &= g_D & \text{on } \Gamma_D, \\ (\kappa \nabla u) \cdot \vec{n} &= g_N & \text{on } \Gamma_N. \end{aligned}$$

Here,  $\vec{n}: \partial\Omega \rightarrow \mathbb{S}^{d-1}$  refers to the unit outer normal on  $\partial\Omega$  (where  $\mathbb{S}^{d-1} \subset \mathbb{R}^d$  is the unit  $(d-1)$ -sphere). By means of Nitsche's method, see [24], one can derive a weak formulation with weak enforcement of the boundary condition for the diffusion problem stated above. We thus define the symmetric bilinear form  $a: V \times V \rightarrow \mathbb{R}$  with  $V := H^1(\Omega)$  for  $u, v \in V$  as

$$a(u, v) := \int_{\Omega} \kappa \nabla u \cdot \nabla v + \rho uv \, dx - \int_{\Gamma_D} (\nabla u \cdot \vec{n}) v \, ds - \int_{\Gamma_D} (\nabla v \cdot \vec{n}) u \, ds + C_{\text{pen}} \int_{\Gamma_D} uv \, ds \quad (1)$$

and the linear functional  $l: V \rightarrow \mathbb{R}$  for  $v \in V$  as

$$l(v) := \int_{\Omega} f v \, dx - \int_{\Gamma_D} (\nabla v \cdot \vec{n}) g_D \, ds + C_{\text{pen}} \int_{\Gamma_D} g_D v \, ds + \int_{\Gamma_N} g_N v \, ds,$$

where  $C_{\text{pen}} > 0$  denotes a penalty parameter used to weakly impose the boundary condition. The corresponding weak formulation of the diffusion problem reads: Find  $u \in V$  such that

$$a(u, v) = l(v) \quad \text{for all } v \in V. \quad (2)$$

A bilinear form  $a: V \times V \rightarrow \mathbb{R}$  is called coercive with coercivity constant  $\alpha > 0$  if it holds

$$a(u, u) \geq \alpha \|u\|_V^2 \quad (3)$$

for all  $u \in V$ . The bilinear form  $a$  is further called continuous if

$$|a(u, v)| \leq \gamma \|u\|_V \|v\|_V \quad (4)$$

for all  $u, v \in V$ . The bilinear form defined in (1) is continuous and coercive for a suitable choice of the penalty parameter  $C_{\text{pen}}$  and, thus, the weak formulation in (2) has a unique solution  $u \in V$  for that choice of the penalty parameter as well, see [3, 31] for more details and a thorough derivation. In practice, the constant  $C_{\text{pen}}$  is typically chosen heuristically since the required lower bounds for this constant are usually not known explicitly. Further, it is well-known that the weak formulation in (2) is equivalent to the energy minimization problem

$$u = \arg \min_{v \in V} I(v) \quad (5)$$

with

$$\begin{aligned} I(v) &:= \frac{1}{2} \int_{\Omega} \kappa \nabla v \cdot \nabla v + \rho v^2 \, dx - \int_{\Omega} f v \, dx \\ &\quad - \int_{\Gamma_D} (\nabla v \cdot \vec{n})(v - g_D) \, ds + \frac{C_{\text{pen}}}{2} \int_{\Gamma_D} v^2 - 2g_D v \, ds - \int_{\Gamma_N} g_N v \, ds \\ &= \frac{1}{2} a(v, v) - l(v). \end{aligned} \quad (6)$$

This energy minimization formulation is also known as *Dirichlet's principle* and it is valid for general weak formulations with symmetric bilinear form. The equivalent formulation of the elliptic PDE in weak form as a minimization problem over the ansatz space  $V$  plays a crucial role in the deep Ritz method.

**Remark 1** (Differences to the formulation in [8]). *We highlight at this point the differences of our weak formulation to the one considered in [8]: Besides the penalty term for the weak enforcement of the boundary condition also present in [8] for homogeneous Dirichlet boundary values, we added a consistency term to the bilinear form and the respective term that leads to a symmetric problem. This way, a strong solution of the diffusion problem is also a weak solution and the weak formulation is consistent with the strong formulation. A similar formulation based on Nitsche's method was also considered in [19] in the context of deep Ritz methods. However, we also incorporated a linear reaction term with non-negative reaction rate  $\rho$  here.*

**Remark 2** (Non-symmetric problems and residual minimization). *The energy minimization formulation as presented here is only valid for symmetric problems. In a more general setting, one might consider the (weak) residual defined in the dual space instead and perform minimization of the residual. The authors in [32] propose to this end the "Deep Double Ritz Method" which solves the corresponding saddle-point problem by means of two deep Ritz minimizations.*

Later on, we will consider approximations of the weak solution  $u \in V$  in subspaces  $V_h \subset V$  of  $V$ . To analyze the error made by the approximation in the subspace  $V_h$ , the following result by Céa gives an error estimate for the so-called *Galerkin projection*  $u_h \in V_h$  by means of the best-approximation error in the space  $V_h$ . Subsequently, the best-approximation error will be bounded further in the case of an approximation via kernel methods.

**Theorem 1** (Céa's Lemma; see [6]). *Let  $V_h \subset V$  be a closed subspace of  $V$ . Further, let  $a: V \times V \rightarrow \mathbb{R}$  be a symmetric, continuous and coercive bilinear form and  $l \in V'$  a continuous linear functional. We denote by  $u \in V$  the weak solution in  $V$  such that it holds  $a(u, v) = l(v)$  for all  $v \in V$ , and by  $u_h \in V_h$  the weak solution in  $V_h$ , i.e. it holds  $a(u_h, v_h) = l(v_h)$  for all  $v_h \in V_h$ . Then the quasi-best approximation estimate*

$$\|u - u_h\|_V \leq \sqrt{\frac{\gamma}{\alpha}} \inf_{v_h \in V_h} \|u - v_h\|_V$$

holds, where  $\gamma > 0$  is the continuity constant, see (4), and  $\alpha > 0$  denotes the coercivity constant of the bilinear form  $a$  with respect to the norm on  $V$ , see (3).

Below we will prove an a priori error estimate for the deep Ritz method using kernel approximations with respect to the  $H^1$ -norm. This result naturally gives rise to an estimate in the  $L^2$ -norm since the  $L^2$ -norm is bounded from above by the  $H^1$ -norm. However, the estimate with respect to the  $L^2$ -norm can be improved further using the well-known Aubin-Nitsche Lemma, which will be recalled in the following in a general and abstract setting.

**Theorem 2** (Aubin-Nitsche Lemma; see [5]). *Let  $V_h \subset V$  be a closed subspace of  $V$  and let  $W$  be a Hilbert space such that the embedding  $V \hookrightarrow W$  is continuous. Further, let the assumptions from Theorem 1 be fulfilled. Then it holds the estimate*

$$\|u - u_h\|_W \leq \gamma \|u - u_h\|_V \sup_{0 \neq w \in W} \frac{\inf_{v_h \in V_h} \|v_w - v_h\|_V}{\|w\|_W},$$

where  $v_w \in V$  is for a given  $w \in W$  defined as the solution of the dual problem

$$a(\varphi, v_w) = (w, \varphi)_W \quad \text{for all } \varphi \in V. \quad (7)$$

## 2.2 Kernel methods and approximation error estimates

Kernel methods constitute a popular machine learning method and are well-known for a comprehensive theoretical foundation, see for instance [34] for a detailed overview. These methods build in our case around the notion of strictly positive-definite kernels, i.e. symmetric functions  $k: \mathbb{R}^d \times \mathbb{R}^d \rightarrow \mathbb{R}$ , for which the kernel matrix  $[k(x_i, x_j)]_{i,j=1}^n \in \mathbb{R}^{n \times n}$  is positive-definite for all sets of pairwise distinct points  $x_1, \dots, x_n \in \mathbb{R}^d$  and all  $n \in \mathbb{N}$ .

From now on, let  $k$  be a radial basis function kernel, i.e. there exists a radial basis function  $\Phi: \mathbb{R}^d \rightarrow \mathbb{R}$  such that  $k(x, y) = \Phi(x - y) = \varphi(\|x - y\|_2)$  with  $\varphi: \mathbb{R}_{\geq 0} \rightarrow \mathbb{R}$  for all  $x, y \in \mathbb{R}^d$ . We assume that for the Fourier transform  $\hat{\Phi}: \mathbb{R}^d \rightarrow \mathbb{R}$  of  $\Phi$  the algebraic decay property

$$c_1(1 + \|\omega\|_2^2)^{-\tau} \leq \hat{\Phi}(\omega) \leq c_2(1 + \|\omega\|_2^2)^{-\tau} \quad \text{for all } \omega \in \mathbb{R}^d \quad (8)$$

holds, where  $c_2 > c_1 > 0$  are some constants and  $\tau > d/2$  is the order of the decay.

For any strictly positive definite kernel  $k$ , there exists a unique Hilbert space  $\mathcal{H}_k$  of functions, the so-called reproducing kernel Hilbert space (RKHS) or native space. Under the assumption (8), the RKHS of  $k$  over a Lipschitz domain  $\Omega$  can be shown to be norm-equivalent to the Sobolev space  $H^\tau(\Omega)$ . We will assume  $\Omega$  to be a Lipschitz domain in the following.

In particular, kernels can be used for interpolation and regression tasks: Given a finite set  $X = \{x_1, \dots, x_n\} \subset \mathbb{R}^d$  with corresponding target values  $y_1, \dots, y_n \in \mathbb{R}$ , the respective approximation task minimizing the mean-square error reads as

$$s_n = \arg \min_{f \in \mathcal{H}_k} \frac{1}{n} \sum_{i=1}^n |y_i - f(x_i)|^2 + \lambda \|f\|_{\mathcal{H}_k}^2,$$

where  $\lambda \geq 0$  denotes a regularization parameter that aims to avoid overfitting of the target data and  $\|\cdot\|_{\mathcal{H}_k}$  is the norm on the Hilbert space  $\mathcal{H}_k$ . A well-known representer theorem, see for instance [14], states that solutions to this optimization problem are of the form

$$s_n = \sum_{j=1}^n \beta_j k(\cdot, x_j), \quad (9)$$

where the coefficients  $\beta_1, \dots, \beta_n \in \mathbb{R}$  define the kernel approximant. When restricting to a pure interpolation task, i.e.  $\lambda = 0$ , the ansatz function  $s_n$  from (9) together with the interpolation conditions  $s_n(x_i) = y_i$  for all  $i = 1, \dots, n$  yield the linear system of equations

$$K\beta = y$$

for the vector of coefficients  $\beta = [\beta_i]_{i=1}^n \in \mathbb{R}^n$ , where  $K \in \mathbb{R}^{n \times n}$  denotes the kernel matrix with entries  $K_{ij} = k(x_i, x_j)$  for  $1 \leq i, j \leq n$  and  $y = [y_1, \dots, y_n]^\top \in \mathbb{R}^n$ . Due to the assumption of  $k$  being strictly positive definite, this linear system of equations admits a unique solution since the kernel matrix  $K$  is positive definite. Kernel based approximation thus takes place in the (finite-dimensional) ansatz space

$$V_{X,k} := \text{span}(k(\cdot, x_i) : x_i \in X) = \text{span}(\Phi(\cdot - x_i) : x_i \in X). \quad (10)$$

In the case of approximation of a function  $f: \Omega \rightarrow \mathbb{R}$ , i.e. the case  $y_1 = f(x_1), \dots, y_n = f(x_n)$ , it is possible to quantify the approximation error between the kernel approximant  $s_n$  and the function  $f$ . To this end, one usually makes use of the mesh norm  $h$  (also called fill distance in the context of scattered data) of the finite set  $X = \{x_1, \dots, x_n\} \subset \Omega$  in  $\Omega \subset \mathbb{R}^d$ , which is defined as

$$h := h_{X,\Omega} := \sup_{x \in \Omega} \min_{x_i \in X} \|x - x_i\|_2.$$

We here use the term “mesh norm” instead of “fill distance” since in our unsupervised learning setting we can place the centers on a uniform mesh in order to reduce the mesh norm. In the context of supervised learning tasks, the data that is to be approximated is usually given and therefore, according to the representer theorem, also the positions of the centers are determined by the data.

With this notation, we state the following approximation error estimate for functions in a Sobolev space by functions from the space  $V_{X,k}$  that was proven in [21]:

**Theorem 3** (Approximation error estimate for kernel methods in Sobolev norms; see [21, Theorem 3.8]). *Let  $k$  be a radial basis function kernel with radial basis function  $\Phi$  satisfying (8) with  $\tau \geq t > d/2$ , let  $\Omega$  satisfy an interior cone condition, and assume that  $X = \{x_1, \dots, x_n\} \subset \Omega$  has mesh norm  $h$  that fulfills (the technical) condition (9) in [21]. If  $u \in H^t(\Omega)$ , then there exists a function  $v \in V_{X,k} = \text{span}(\Phi(\cdot - x_i) : x_i \in X)$  such that for every real  $0 \leq r \leq t$  it holds*

$$\|u - v\|_{H^r(\Omega)} \leq Ch^{t-r} \|u\|_{H^t(\Omega)},$$

where  $C$  is a constant independent of  $u$  and  $h$ .

Theorem 3 provides a bound on the error when approximating functions in a Sobolev space by functions from the subspace  $V_{X,k}$ . In the context of kernel methods one is usually interested in interpolation error estimates where the function  $v \in V_{X,k}$  is chosen as the interpolant of the function  $u$  in the centers. However, in the following section we consider an unsupervised learning approach where the approximation  $v \in V_{X,k}$  is not an interpolant but a quasi-best approximation of  $u$ . For the a priori error estimates we therefore need a bound for the best approximation error by functions in  $V_{X,k}$  which is provided by Theorem 3. Certainly, interpolation error estimates, see for instance [22], also provide an upper bound for the best approximation error, but these estimates tend to be less effective when the points in  $X$  are closely spaced. We thus resort to an approximation error estimate which fits to the proof of Theorem 4 based on Céa’s Lemma. We also remark that in the context of finite element methods, error estimates for interpolations of functions from Sobolev spaces by functions from finite element spaces are used to prove a priori error estimates.

### 3 Application of kernel approximations in the deep Ritz method

The main idea of the deep Ritz method, introduced in [8], is to apply deep neural networks as ansatz functions in the energy minimization problem for the functional  $I$  from (6). For the minimization, standard optimization algorithms from the machine learning literature, such as stochastic gradient descent, can be employed. The method has been investigated regarding its convergence in [20] using the notion

of  $\Gamma$ -convergence. However, a priori error estimates for the approach are typically intricate to derive, see [18, 12].

Instead of using deep neural networks, we consider kernel approximations as introduced in Section 2.2 as ansatz functions. We would like to emphasize at this point again that for a fixed kernel  $k$  and fixed centers  $X = \{x_1, \dots, x_n\}$ , the set of kernel functions for different coefficients forms the linear space  $V_{X,k}$  as introduced in (10). This is not the case for the set of neural networks with different weights when considering a fixed neural network architecture, which does not form a linear space. Hence, for instance Céa's Lemma, see Theorem 1, cannot be applied to the set of neural networks.

The application of kernel methods instead of neural networks in the deep Ritz approach is motivated by the available theoretical results that will be established in Section 3.2. For sufficiently regular solutions we further expect satisfactory numerical results, see Section 4. Furthermore, the formulation as an energy minimization problem instead of a linear system of equations (resulting from the weak equation in (2)) has several advantages when using kernel approximants as ansatz functions. First of all, the entries of the stiffness matrix  $A \in \mathbb{R}^{n \times n}$  using the space  $V_{X,k}$  as ansatz and test space are given for  $i, j = 1, \dots, n$  as

$$A_{ij} = a(k(\cdot, x_j), k(\cdot, x_i)). \quad (11)$$

This matrix could be subsequently used to solve (2) in the subspace  $V_{X,k}$  via

$$A\boldsymbol{\beta} = \ell \quad (12)$$

to determine the approximant  $s_n = \sum_{j=1}^n \beta_j k(\cdot, x_j)$  with coefficients  $\boldsymbol{\beta} = [\beta_i]_{i=1}^n \in \mathbb{R}^n$  and right-hand side vector  $\ell = [\ell(k(\cdot, x_i))]_{i=1}^n \in \mathbb{R}^n$ .

We observe that this matrix has a similar structure than the kernel matrix  $K$  in the sense that both can be seen as Gramian matrices. It has been discussed theoretically in [7], and we also observe this issue numerically below, that the stiffness matrix  $A$  of the weak formulation might be ill-conditioned when using kernels as ansatz and test functions. This results in difficulties when solving linear systems with the stiffness matrix. Additionally, computing the entries of the stiffness matrix is challenging due to the required accurate numerical quadrature. In finite element methods, the ansatz and test functions have support only on a small number of elements and are usually polynomials of moderate degree, which enables an exact computation of the required integrals (as long as the data functions can also be integrated exactly). Another drawback of the linear system is that the stiffness matrix might be dense in the kernel-based approach. Hence, solving the linear system is not only difficult due to the large condition number of the system matrix but is also costly because the stiffness matrix is not sparse. This is again in contrast to finite element methods where the ansatz functions have compact support and the resulting system can be solved very efficiently by means of iterative methods. However, using the formulation of the weak problem via the energy minimization, we can circumvent the issues described before. We will discuss these advantages in detail based on numerical examples in Section 4.

### 3.1 Description of the method

In the following, we describe the deep Ritz approach using kernel methods in more detail. To this end, assume that we are given a fixed set of points  $X = \{x_1, \dots, x_n\} \subset \Omega$  and a kernel  $k$ . We denote by  $u_h \in V_h = V_{X,k} \subset H^1(\Omega)$  the weak solution of the variational problem (2) considered over the space  $V_{X,k}$ , which will be computed by minimizing the energy functional from (6), i.e. we have

$$u_h = \arg \min_{v_h \in V_{X,k}} I(v_h). \quad (13)$$

The subscript  $h$  refers to the mesh norm that will also appear in the a priori error estimate and can be seen as the discretization parameter of the space  $V_{X,k}$  with respect to the space  $V$ . In that sense, the mesh norm has a similar meaning as the grid size in finite element methods.

As before, for a fixed set  $X = \{x_1, \dots, x_n\}$ , we consider ansatz functions  $\psi_h[\boldsymbol{\beta}] \in V_{X,k}$  of the form

$$\psi_h[\boldsymbol{\beta}](x) = \sum_{i=1}^n \beta_i k(x, x_i) \quad (14)$$

for  $x \in \Omega$  with coefficient vector  $\beta = [\beta_i]_{i=1}^n \in \mathbb{R}^n$ . The optimization problem in (13) can thus be rewritten as

$$\beta^* = \arg \min_{\beta \in \mathbb{R}^n} I(\psi_h[\beta]) \quad (15)$$

and  $u_h$  is then given as  $u_h = \psi_h[\beta^*]$ . In other words, given a kernel and a set of centers, we search for coefficients such that the linear combination of the kernel centered at the given center points (as given in (14)) minimizes the energy functional. Due to the equivalence of the variational formulation and the energy minimization problem, solving (15) exactly results in the weak solution of the variational problem (2) over the space  $V_{X,k}$ , i.e. it holds

$$a(u_h, v_h) = l(v_h) \quad \text{for all } v_h \in V_{X,k}.$$

After a suitable discretization of the energy functional  $I$ , we can solve the optimization problem in (15) for the optimal coefficients using standard gradient-based methods from the machine learning literature, see Section 3.3 for details on the practical implementation of the method.

We emphasize at this point that we consider weak boundary values within the weak formulation in (2). This is similar to the original deep Ritz method using neural networks as ansatz functions. Applying kernel approximants instead of neural networks results in the same difficulty that strong boundary values are virtually impossible to prescribe for these kinds of functions. We thus proceed with a similar weak boundary value enforcement as performed in [8].

Due to the linear structure of the ansatz space  $V_{X,k}$  and the thorough approximation error analysis available for kernel methods, it is possible to derive a priori error estimates for the solution  $u_h \in V_{X,k}$  of the energy minimization problem. Such error estimates with respect to different norms are presented in the next section.

### 3.2 A priori error estimation

Using the theoretical results on weak formulations and on approximation errors for kernel methods, we now formulate an a priori error estimate with respect to the  $H^1$ -norm for the error of the kernel based solution  $u_h \in V_{X,k}$  from Section 3. Having the theoretical tools from the previous sections at hand, the proof of the error estimate is relatively simple and follows the standard procedure for deriving a priori error estimates for weak solutions of elliptic PDEs. The error estimate is also similar to the one for Lagrange finite elements of order  $m - 1$  where  $h$  denotes the grid size of the triangulation. We highlight at this point as well that the result holds similarly for arbitrary weak formulations which are equivalent to energy minimization problems.

**Theorem 4** (A priori error estimate in the  $H^1$ -norm). *Let  $\Omega \subset \mathbb{R}^d$  be a bounded domain and assume that  $\Omega$  satisfies an interior cone condition. Let  $V = H^1(\Omega)$ , let  $a: V \times V \rightarrow \mathbb{R}$  be a symmetric, continuous and coercive bilinear form, and let  $l \in V'$  be a continuous linear functional on  $V$ . Furthermore, let  $u \in V$  be the weak solution of the variational problem (2). Assume that the positive definite radial basis function kernel  $k: \Omega \times \Omega \rightarrow \mathbb{R}$  has an algebraically decaying Fourier transform of order  $\tau \geq m > d/2$  for some  $m \in \mathbb{R}$ , i.e. it holds (8) with  $\tau$  given as stated before. Let  $X = \{x_1, \dots, x_n\} \subset \Omega$  have mesh norm  $h > 0$  such that condition (9) in [21] is fulfilled. Assuming  $u \in H^m(\Omega)$ , we have that there exists a constant  $c_{H^1} > 0$  independent of  $h$  and  $l$  such that for the kernel approximation  $u_h \in V_h = V_{X,k} \subset V$ , which solves the energy minimization problem in eq. (13), it holds*

$$\|u - u_h\|_{H^1(\Omega)} \leq c_{H^1} h^{m-1} \|u\|_{H^m(\Omega)}.$$

*Proof.* We first note that since  $u_h \in V_{X,k}$  solves the energy minimization problem, it is also the unique weak solution of the variational problem  $a(u_h, v_h) = l(v_h)$  for all  $v_h \in V_{X,k}$  according to Dirichlet's principle, see Section 2.1. Therefore, applying first Céa's Lemma with  $V_h = V_{X,k}$ , see Theorem 1, and then the approximation error estimate from Theorem 3 with  $\tau = t = m$  and  $r = 1$ , we obtain

$$\begin{aligned} \|u - u_h\|_{H^1(\Omega)} &\leq \sqrt{\frac{\gamma}{\alpha}} \inf_{v_h \in V_{X,k}} \|u - v_h\|_{H^1(\Omega)} \\ &\leq C \sqrt{\frac{\gamma}{\alpha}} h^{m-1} \|u\|_{H^m(\Omega)} \\ &\leq c_{H^1} h^{m-1} \|u\|_{H^m(\Omega)} \end{aligned}$$

with  $c_{H^1} := C\sqrt{\frac{\tau}{\alpha}}$ , which proves the theorem.  $\square$

**Remark 3** (Differences to the a priori error estimate in [33]). *In Corollary 5.4 in [33], it was necessary to assume  $m > d/2 + 1$ . Since this is not required in the approximation error estimate in Theorem 3, we can weaken the assumption to  $m > d/2$  in the a priori error estimate as well. We emphasize at this point that Theorem 4 in particular implies that the radial basis function kernel  $k$  is allowed to have a higher regularity (i.e.  $\tau > m$ ) than the solution  $u \in H^m(\Omega)$  itself. In contrast, standard interpolation error estimates for Lagrange finite elements typically require that the solution has a higher regularity than the polynomial degree of the ansatz functions.*

We now also derive an error estimate with respect to the  $L^2$ -norm that obtains the optimal order of convergence (i.e. order  $m$  instead of order  $m - 1$  as for the  $H^1$ -norm). To that end, we combine the previous  $H^1$ -estimate with the Aubin-Nitsche Lemma from Theorem 2 and obtain the following result:

**Theorem 5** (A priori error estimate in the  $L^2$ -norm). *Let the assumptions from Theorem 4 be fulfilled. Assume further that it holds  $m \geq 2$  and that for every  $w \in L^2(\Omega)$  the solution of the dual problem (7) satisfies  $v_w \in H^2(\Omega)$  and  $\|v_w\|_{H^2(\Omega)} \leq \bar{C} \|w\|_{L^2(\Omega)}$  for some fixed constant  $\bar{C} > 0$ . Then there exists a constant  $c_{L^2} > 0$  such that the estimate*

$$\|u - u_h\|_{L^2(\Omega)} \leq c_{L^2} h^m \|u\|_{H^m(\Omega)}$$

holds.

*Proof.* We apply the Aubin-Nitsche Lemma from Theorem 2 with  $V = H^1(\Omega)$  and  $W = L^2(\Omega)$ . We can hence estimate

$$\begin{aligned} \|u - u_h\|_{L^2(\Omega)} &\leq \gamma \|u - u_h\|_{H^1(\Omega)} \sup_{0 \neq w \in L^2(\Omega)} \frac{\inf_{v_h \in V_h} \|v_w - v_h\|_{H^1(\Omega)}}{\|w\|_{L^2(\Omega)}} \\ &\leq \gamma c_{H^1} h^{m-1} \|u\|_{H^m(\Omega)} \sup_{0 \neq w \in L^2(\Omega)} \frac{Ch \|v_w\|_{H^2(\Omega)}}{\|w\|_{L^2(\Omega)}} \\ &\leq \gamma c_{H^1} h^{m-1} \|u\|_{H^m(\Omega)} \sup_{0 \neq w \in L^2(\Omega)} \frac{C\bar{C}h \|w\|_{L^2(\Omega)}}{\|w\|_{L^2(\Omega)}} \\ &= c_{L^2} h^m \|u\|_{H^m(\Omega)} \end{aligned}$$

with  $c_{L^2} := \gamma c_{H^1} C\bar{C}$ , where we made use of the result in the  $H^1$ -norm from Theorem 4 and the approximation error from Theorem 3 to bound the approximation error of the dual solution  $v_w$ .  $\square$

The theoretical results obtained in this section provide estimates of the approximation error achieved by the kernel approximation of the weak solution in terms of the mesh norm  $h$ . We observe that, compared to finite element methods, a relatively high degree of regularity of the weak solution  $u$  is required for the results to hold. The necessary regularity is closely related to the conditions under which approximation error estimates for kernel approximants are valid. Further, we see that the convergence rate of the approximation via kernel approaches is restricted by the regularity of the kernel or the solution. Indeed, if the kernel has a higher regularity than the solution, i.e.  $\tau > m$ , the convergence rate is limited by the regularity of the solution. This case is often referred to as “escaping the native space”. Conversely, if the kernel is less smooth than the solution, i.e.  $\tau < m$ , the order of convergence is usually limited by the regularity of the kernel. This behavior will also be discussed in the numerical experiments shown below. We further emphasize that the convergence rates are similar as for kernel interpolation of the true solution since the minimizer of the energy functional is a quasi-best approximation of the weak solution according to Céa’s Lemma. We hence obtain a solution whose performance in terms of approximation error with respect to the weak solution is similar to the kernel interpolant without requiring access to the function that is to be interpolated.

The a priori error estimates imply in particular that, from a theoretical perspective, reducing the mesh norm by increasing the number of centers in a suitable way results in smaller approximation errors. Moreover, depending on the smoothness of the weak solution, employing a kernel with higher regularity leads to improved convergence rates. Such statements on how to improve the accuracy of the method are



typically not available when considering neural networks as ansatz functions. Approaches based on neural networks often lack strategies for systematically adjusting the architecture (number of layers, number of neurons, activation function, etc.) in order to obtain a certain approximation quality.

We conclude the section with a remark on how to derive upper bounds independent of the norm of the weak solution.

**Remark 4** (Estimates depending only on the problem data). *To obtain a priori bounds that are independent of the weak solution  $u \in H^m(\Omega)$  but only depend on the data of the problem, that is, on the bilinear form and the right hand side, one can use regularity results for weak formulations of boundary-value problems similar to the one assumed in Theorem 5, see for instance [9, Chapter 6.3].*

### 3.3 Practical aspects

For the practical implementation of the deep Ritz method with kernel functions, one has to approximate the bilinear form  $a$  and the linear functional  $l$  occurring in the energy minimization problem. In most applications, the variational formulation is motivated by the weak formulation of a PDE and thus consists of integrals of the ansatz and test functions or their derivatives over the domain  $\Omega$ . These integrals can usually not be evaluated exactly, in particular not for arbitrary kernel functions as ansatz functions. One therefore deals with a bilinear form  $a_{h_{\text{int}}} : V_h \times V_h \rightarrow \mathbb{R}$  and a linear functional  $l_{h_{\text{int}}} \in V_h'$  that involve a numerical quadrature and constitute approximations to  $a$  and  $l$ , respectively. To obtain an a priori error estimate in the situation where  $u_h \in V_h$  solves the energy minimization problem for the approximate energy functional  $I_{h_{\text{int}}} : V_h \rightarrow \mathbb{R}$ , defined for  $v_h \in V_h$  as  $I_{h_{\text{int}}}(v_h) := \frac{1}{2}a_{h_{\text{int}}}(v_h, v_h) - l_{h_{\text{int}}}(v_h)$ , it is possible to apply Strang's Lemma, see [29], where the error introduced by the quadrature rule can be taken into account.

Besides the approximation of the energy functional, the optimization problem in (15) can usually be solved only approximately. In the following Lemma, we give a bound on the approximation error in terms of the difference in the objective function value.

**Lemma 1** (Inexact solution of the optimization problem). *Let us denote by  $u_h \in V_{X,k} \subset V$  the solution of (13). Let us further denote by  $\tilde{u}_h \in V_{X,k}$  an approximation of  $u_h$ . Then it holds that*

$$\|u_h - \tilde{u}_h\|_V^2 \leq \frac{I(\tilde{u}_h) - I(u_h)}{\alpha - \frac{\gamma}{2}},$$

where  $\alpha$  and  $\gamma$  denote the coercivity and continuity constants of  $a$ , respectively.

*Proof.* Due to the coercivity, symmetry and continuity of  $a$ , as well as the assumption that  $u_h$  is a weak solution, it holds

$$\begin{aligned} \alpha \|u_h - \tilde{u}_h\|_V^2 &\leq a(u_h - \tilde{u}_h, u_h - \tilde{u}_h) \\ &= a(u_h, u_h) - 2a(u_h, \tilde{u}_h) + a(\tilde{u}_h, \tilde{u}_h) \\ &= l(u_h) - l(\tilde{u}_h) - a(u_h, \tilde{u}_h) + a(\tilde{u}_h, \tilde{u}_h) \\ &= I(\tilde{u}_h) + l(u_h) - \frac{1}{2}a(u_h, u_h) + \frac{1}{2}a(u_h, u_h) - a(u_h, \tilde{u}_h) + \frac{1}{2}a(\tilde{u}_h, \tilde{u}_h) \\ &= I(\tilde{u}_h) - I(u_h) + \frac{1}{2}a(u_h - \tilde{u}_h, u_h - \tilde{u}_h) \\ &\leq I(\tilde{u}_h) - I(u_h) + \frac{\gamma}{2} \|u_h - \tilde{u}_h\|_V^2. \end{aligned}$$

It hence holds

$$\left(\alpha - \frac{\gamma}{2}\right) \|u_h - \tilde{u}_h\|_V^2 \leq I(\tilde{u}_h) - I(u_h).$$

Dividing by  $\alpha - \frac{\gamma}{2}$  yields the claimed result.  $\square$

The previous Lemma provides a bound on how an inexact solution of the optimization problem in (15) can affect the approximation quality. If the optimization problem is solved accurately, i.e.  $I(\tilde{u}_h) - I(u_h)$  is small, the approximation error of  $\tilde{u}_h$  compared to  $u_h$  is small as well. However, it is important to

note that the error of  $\tilde{u}_h$  with respect to the norm on  $V$  is bounded by the square root of the difference in the objective function values. For a prescribed approximation error  $\varepsilon > 0$ , one thus has to solve the optimization problem up to a tolerance of  $\varepsilon^2$ .

Lemma 1 can be combined with Theorems 4 and 5 to obtain the following error bounds by means of the triangle inequality:

**Proposition 1** (A priori error estimates with inexact solution of the optimization problem). *Let the assumptions from Theorems 4 and 5 and Lemma 1 be fulfilled. Then we have that*

$$\|u - \tilde{u}_h\|_{H^1(\Omega)} \leq c_{H^1} h^{m-1} \|u\|_{H^m(\Omega)} + \left( \frac{I(\tilde{u}_h) - I(u_h)}{\alpha - \frac{\gamma}{2}} \right)^{1/2}$$

and

$$\|u - \tilde{u}_h\|_{L^2(\Omega)} \leq c_{L^2} h^m \|u\|_{H^m(\Omega)} + \left( \frac{I(\tilde{u}_h) - I(u_h)}{\alpha - \frac{\gamma}{2}} \right)^{1/2}.$$

In the next section we present two numerical examples in which we investigate the behavior of kernel methods in the deep Ritz framework and verify our theoretical convergence results in practice.

## 4 Numerical experiments

In this section we first discuss some implementational details and give additional information on the parameters used in our numerical examples. Afterwards, we present two different test cases in two spatial dimensions. First of all, we consider a problem where the solution is smooth such that the convergence rate of the deep Ritz approach using kernel methods is determined by the smoothness of the kernel. We will investigate this dependency of the convergence rate in detail and compare the results to our theoretical findings. Afterwards, we consider an example with a singular solution where we expect the convergence rates to be determined by the regularity of the solution independent of the smoothness of the kernel.

### 4.1 Implementational details

In order to (approximately) solve the optimization problem in (15), it is possible to apply gradient-based methods such as the Adam optimizer [15] that is used in our numerical experiments. Various learning rate schedulers from the machine learning literature can further be used to adjust the step size within the gradient descent method. Below, we consider a learning rate scheduler that reduces the learning rate by a certain factor at prescribed milestones, i.e. after given numbers of training epochs. We perform up to 100.000 epochs and the learning rate scheduler reduces the learning rate by a factor of 0.5 up to 15 times. We make use of the PyTorch library [25] and compute the gradient of the energy functional using automatic differentiation [1].

The integrals in the energy functional (6) are approximated using Monte Carlo integration. The quadrature points are drawn randomly in every epoch, which corresponds to random mini-batching in the machine learning literature. We use in particular more quadrature points than centers and therefore ensure  $h_{\text{int}} < h$ , see Section 3.3 as well. To be more precise, Monte Carlo quadrature has a convergence rate of  $\mathcal{O}(N^{-1/2})$  for  $N$  uniformly distributed points. Hence, the choice  $N \sim h^{-2(m+1)}$  leads to the same error rate as in Theorem 4 by Strang's Lemma. However, this choice for the number of quadrature points is impractical already for moderate values of the mesh norm  $h$  and smoothness  $m$ . We therefore choose a new quadrature point set of moderate size randomly in each epoch instead of generating a large set that is fixed during the whole optimization loop. For the numerical experiments, we focus on the class of Matérn kernels [34] of different smoothness, which have an algebraic decay of the Fourier transform according to (8). The regularity of Matérn kernels is determined by a parameter  $\nu > 0$ . For  $\nu = p + \frac{1}{2}$  with  $p \in \mathbb{N}$ , Matérn kernels possess a simplified expression as a product of an exponential and a polynomial of degree  $p$ . Hence, we consider in the following Matérn kernels for  $\nu \in \{1/2, 3/2, 5/2\}$ , which correspond to an algebraic decay of the Fourier transform of order  $\tau = \nu + \frac{d}{2}$ , see (8). Since we apply our approach to numerical examples in two dimensions, the order  $\tau$  is given as  $\tau = \nu + 1 \in \{3/2, 5/2, 7/2\}$ . The

$p$	$\nu$	$\tau$	Convergence rate		Convergence rate	
			for regularity $m \geq \tau$		for regularity $m < \tau$	
			$H^1$ -norm	$L^2$ -norm	$H^1$ -norm	$L^2$ -norm
0	1/2	3/2	1/2	3/2	$m - 1$	$m$
1	3/2	5/2	3/2	5/2	$m - 1$	$m$
2	5/2	7/2	5/2	7/2	$m - 1$	$m$

Table 1: Regularity of Matérn kernels for  $d = 2$  with different parameters and convergence rates depending on the smoothness  $\tau$  of the kernel and the regularity  $m$  of the weak solution, i.e.  $k$  has an algebraically decaying Fourier transform of order  $\tau$  and we have  $u \in H^m(\Omega)$ . For the convergence rates with respect to the  $L^2$ -norm we disregard the assumption  $m \geq 2$  from Theorem 5 in the overview in this table.

mentioned relations regarding the regularity of the kernels together with the expected convergence rates according to Theorems 4 and 5 are summarized in Table 1.

We also tested compactly supported kernels of finite smoothness such as the family of Wendland kernels which gave quantitatively the same results in terms of convergence rates. For improved convergence of the optimization, a change of basis of  $V_{X,k}$  to a Lagrange basis was done prior to the optimization. We consider the minimization of the energy functional (6) where the penalty parameter was set to  $C_{\text{pen}} = 100$  for both of the following examples, similar as in [8]. The integrals that occur in the computation of errors are approximated by a uniform quadrature on the domain  $\Omega$  using 10.201 quadrature points. We further depict relative errors of the form  $\|u - u_h\| / \|u\|$ , where  $u$  denotes the exact solution and  $u_h$  the considered approximation. The norm  $\|\cdot\|$  refers either to the  $L^2$ -norm or the  $H^1$ -norm.

In our numerical experiments in the next sections we also compare the approach of using kernel approximants to the original deep Ritz method with neural networks. To this end, we trained fully-connected neural networks with two hidden layers and different numbers of neurons per layer. The hyperbolic tangent was employed as activation function in the neural networks. Since typically no measure for spatial discretization in the context of neural networks that is comparable to the mesh norm for kernel methods is available, we use the number of parameters in order to compare both approaches. In the case of kernel methods, the number of parameters refers to the expansion size, i.e. the number of centers. For neural networks, weights and biases are seen as parameters. The neural networks are trained similarly to the kernel methods using the Adam optimizer with 100.000 iterations and the same learning rate scheduling.

The source code used to carry out the numerical experiments presented in this contribution can be found in [16] and can be used to reproduce the results shown below<sup>1</sup>.

## 4.2 Diffusion equation with a solution of high regularity

As a first test case we consider the following Poisson problem with inhomogeneous Dirichlet boundary conditions:

$$\begin{aligned} -\Delta u &= f && \text{in } \Omega, \\ u &= g && \text{on } \partial\Omega, \end{aligned} \tag{16}$$

where  $\Omega = (0, 1)^2$ ,  $f(x) = 4$  and  $g(x) = 1 - x_1^2 - x_2^2$  for  $x = (x_1, x_2) \in \Omega$ . As can be easily verified, the strong solution of this problem is given as  $u = g$ . This problem thus possesses a solution with arbitrary high smoothness and we therefore expect that the convergence rate of the kernel approximation is limited by the regularity of the kernel, see Theorem 4.

Moreover, we consider  $n \in \{1, 2, 4, 6, 8, 10, 12, 14, 16, 18, 20\}$  centers per dimension in the interior of the domain  $\Omega$  and add  $4n + 4$  points on the boundary. The centers are placed on a uniform mesh which results in a mesh norm that scales like  $h \sim 1/(n + 1)$  for  $n \in \mathbb{N}$  inner centers per dimension.

Figure 1 depicts the errors of the deep Ritz method using Matérn kernels of different smoothness in the  $L^2$ -norm and the  $H^1$ -norm. In addition, we also present the interpolation errors when considering the same set of centers as for the corresponding deep Ritz method and interpolating the true solution of (16)

<sup>1</sup>The corresponding GitHub-repository containing the source code is available at <https://github.com/HenKlei/KERNEL-DEEP-RITZ>

in these centers. For the interpolation error curves we further show an estimate of the convergence order using a linear regression of the data points.

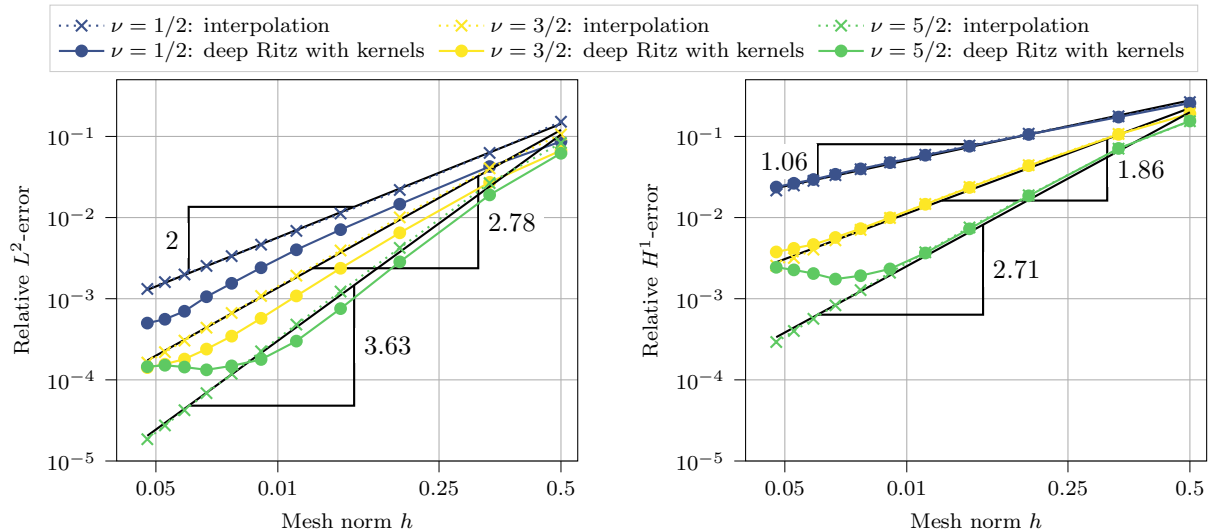


Figure 1: Relative errors in the  $L^2$ -norm (left) and the  $H^1$ -norm (right) with respect to the mesh norm  $h$  for Matérn kernels of smoothness  $\nu \in \{1/2, 3/2, 5/2\}$  in the example with a smooth solution. The dashed lines indicate the error decays of the interpolation of the exact solution by the respective kernel. The estimated convergence rates for the interpolated solutions are shown as black lines.

We observe that the interpolation of the exact solution and the approximation obtained using the deep Ritz approach show the same asymptotical converge rate. Only for  $k = 2$  and a small mesh norm of less than 0.01, the error of the deep Ritz solution stagnates and does not decrease further when adding more centers. We expect that this issue can be circumvented with more advanced learning rate scheduling. We further notice that the  $L^2$ -error of the deep Ritz solution is smaller than the interpolation error in most cases. The deep Ritz solution is a quasi-best approximation with respect to the  $H^1$ -norm whereas the interpolation only considers values of the exact solution at the centers. Approximating the weak solution by means of the deep Ritz solution therefore takes much more information into account in its construction. Moreover, the approximation error can indeed be smaller than the interpolation error, see also the discussion after Theorem 3. Certainly, the interpolation serves solely as a reference here. In practice, the exact solution is usually unknown and it is impossible to compute its interpolation.

In this example the solution is smooth and we have in particular that  $m > \tau$  for the considered values of  $\tau$ . For instance for  $\nu = 1/2$ , we therefore expect a convergence rate of  $3/2$  with respect to the  $L^2$ -norm according to Table 1. Indeed we observe in Figure 1 a convergence rate of about 2, i.e. an additional rate of  $1/2$ . This effect is an instance of superconvergence, see [28], which is a known phenomenon occurring in the context of kernel based approximation when the function that is approximated is much smoother than the kernel itself. We thus obtain higher convergence rates as predicted by the theory in both norms and for all values of  $\nu$ .

In Figure 2 we present a comparison of the errors when using neural networks or Matérn kernels with regularity parameter  $\nu = 3/2$  in the deep Ritz method. The relative errors of the neural networks are about one order of magnitude larger in comparison to those obtained by the kernel models. In particular for small numbers of parameters the neural networks seem to lack the expressivity in order to provide errors comparable to the kernel approach. However, we also observe that in contrast to the error of the kernel methods, the errors of the neural networks still decrease further significantly when increasing the number of parameters in the network.

We further consider the results obtained when assembling the stiffness matrix in (11) as well as the right-hand side and solve the system (12). As mentioned in Section 3, the stiffness matrix suffers from a large condition number which results in problems when solving the associated linear system. The relative errors with respect to the mesh norm when applying Matérn kernels with different smoothness are shown in Figure 3.

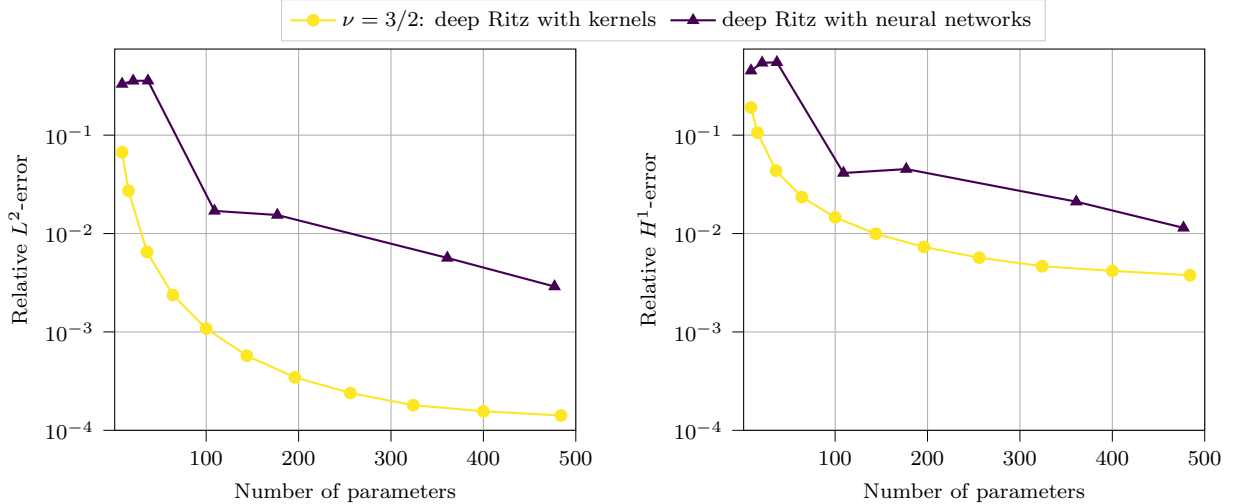


Figure 2: Relative errors in the  $L^2$ -norm (left) and the  $H^1$ -norm (right) with respect to the number of parameters for Matérn kernels of smoothness  $\nu = 3/2$  and fully-connected neural networks in the example with a smooth solution.

We observe that already for mesh norms of about 0.01 the solution obtained by solving the linear system are worse than those computed by the deep Ritz method. For smaller mesh sizes, the relative errors even start to increase which results in an error that is roughly three orders of magnitude larger than the corresponding error of the deep Ritz solution. Moreover, this behavior is the same independent of the smoothness of the kernel. For  $\nu = 5/2$  the problem is even more pronounced than for  $\nu = 1/2$  or  $\nu = 3/2$ . The condition numbers of the stiffness matrix range from  $4 \cdot 10^3$  (for  $\nu = 1/2$  and  $n = 1$ ) to  $2.4 \cdot 10^{19}$  (for  $\nu = 5/2$  and  $n = 20$ ). Solving a linear system with the ill-conditioned stiffness matrix thus constitutes an issue for the linear solver resulting in inaccurate approximations as apparent from Figure 3.

In summary, the deep Ritz method using kernels provides superior results in terms of approximation errors compared to neural networks with a similar number of parameters for this example with a smooth solution. Moreover, by using the formulation as an energy minimization problem we are able to circumvent the issue of a large condition number that arises when assembling the stiffness matrix. The computational effort is further comparable for all methods discussed in this section.

### 4.3 Singular solution on a non-convex domain

In the previous example, the solution was smooth and thus the convergence rate of the deep Ritz method using kernels was limited by the regularity of the applied kernel. Here, we now consider a problem where the solution is singular and the convergence rate is determined by the smoothness of the weak solution of the PDE. Let  $\Omega \subset \mathbb{R}^2$  be a non-convex domain defined as

$$\Omega = \{(r \cos(\varphi), r \sin(\varphi)) \in \mathbb{R}^2 : 0 < r < 1.5, 0 < \varphi < \alpha\} \subset \mathbb{R}^2.$$

We further consider the same diffusion problem as in (16) for  $f(x) = 0$  and

$$g(x) = \|x\|_2^{1/\alpha} \cdot \sin\left(\frac{\arctan(x_2/x_1)}{\alpha}\right) + 1$$

for  $x = (x_1, x_2) \in \bar{\Omega}$ . The solution is again given as  $u = g$ . We set the angle to  $\alpha = \frac{3\pi}{2}$ . Then, we have  $u \in H^{\frac{2}{3\pi}+1-\varepsilon}(\Omega)$  for all  $0 < \varepsilon \leq \frac{2}{3\pi} + 1$  and  $u \notin H^l(\Omega)$  for  $l \geq \frac{2}{3\pi} + 1 \approx 1.2122$ . A plot of the exact solution is shown in Figure 4.

Similar to the previous example we consider  $n \in \{1, 2, 4, 6, 8, 10, 12, 14, 16, 18, 20\}$  centers per dimension in the square  $[-1.5, 1.5]^2$  and remove those centers that are not in the interior of the domain  $\Omega$ . Further, we add  $4n + 4$  points on the boundary  $\partial\Omega$ .

Figure 5 shows the decay of the relative  $L^2$ -error when using Matérn kernels of different smoothness to approximate the singular solution. As we are in the “escaping the native space” case (smoothness of the

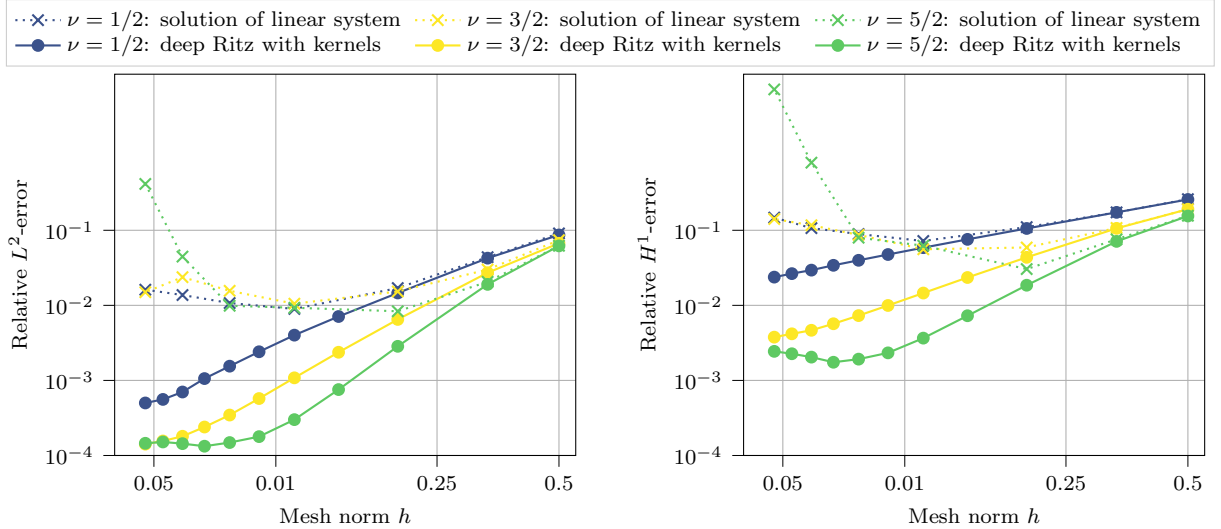


Figure 3: Relative errors in the  $L^2$ -norm (left) and the  $H^1$ -norm (right) with respect to the mesh norm  $h$  for Matérn kernels of smoothness  $\nu \in \{1/2, 3/2, 5/2\}$  using the energy minimization problem and the linear system of equations in the example with a smooth solution.

solution smaller than smoothness of the kernel), we expect the error to decay according to the smoothness of the solution and independent of the smoothness of the kernel function. This behavior can be observed in Figure 5, as the three plots for the different degrees of smoothness follow the same asymptotic. We observe a decay rate of the error with respect to the  $L^2$ -norm of 1.24 which agrees with the regularity of the solution  $u$  of about 1.21. Similarly as in the previous example, the decay rate with respect to the  $H^1$ -norm is one order smaller than for the  $L^2$ -norm. The superconvergence that was present in the previous example cannot be observed here since the exact solution has a lower regularity than the kernels. However, although the solution is singular, it can still be approximated accurately by smooth kernels.

In the beginning (for mesh norms between  $2 \cdot 10^{-2}$  and  $5 \cdot 10^{-2}$ ) one can observe a preasymptotic behavior, which is due to the small amount of centers that is not sufficient to properly cover the domain. The results in Figure 5 also show again that the solution obtained by the deep Ritz method results in smaller errors compared to the interpolation of the exact solution.

In Figure 6 we depict the relative errors for neural networks and Matérn kernels with  $\nu = 3/2$  when used in the deep Ritz method. In this example, the kernel approximants and the neural networks perform quite similar. The  $H^1$ -error of the neural networks is slightly smaller compared to the kernel methods.

Finally, we again investigate the performance of the solution computed by solving the weak formulation via the linear system in (12). In Figure 7 we compare the results to the energy minimization approach using kernels. The errors of both approaches, based on the linear system and the energy optimization, decay at the same rate. Compared to the example in Section 4.2 we further observe that only for the smallest mesh norm and  $\nu = 5/2$  the error of the solution based on the linear system is much larger. The condition numbers in this example vary between  $2.5 \cdot 10^2$  and  $7.9 \cdot 10^{16}$ . However, in this example the effect seems to be less pronounced compared to the example with a smooth solution.

This example shows that the deep Ritz method using kernels as ansatz functions can also be applied in settings where the weak solution has only low regularity. Furthermore, the convergence rate is not influenced by the smoothness of the kernel in this case, which allows to apply kernels with high smoothness as well. We observed that the kernel methods performed similar as the neural networks in this case of a singular solution. However, we emphasize again that the observed convergence rate is underpinned by our theoretical results from Section 3.2.

## 5 Conclusion and outlook

In this contribution we proposed the application of kernel methods as ansatz functions in the deep Ritz approach and analyzed its behavior theoretically as well as numerically. In the original work [8] where

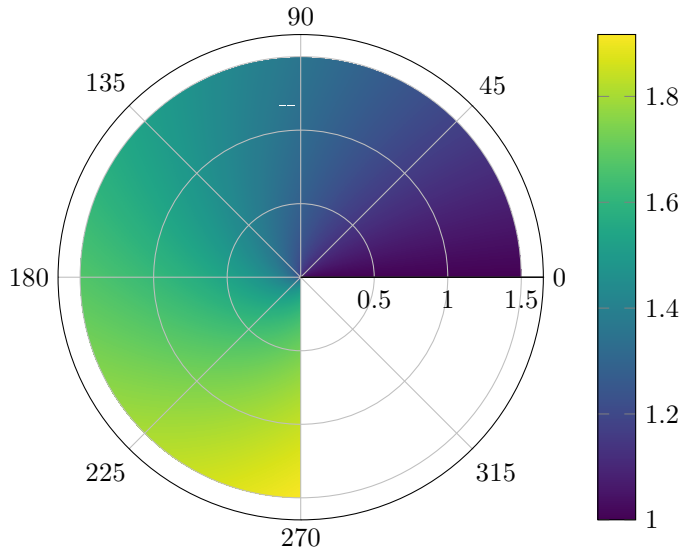


Figure 4: Top view plot of the exact solution in the example with a non-convex domain resulting in a singular solution. The singularity occurs in the origin due to steep gradients.

the deep Ritz approach was proposed, the authors used deep neural networks and optimized the weights of the networks via minimization of an energy functional that is equivalent to the weak formulation of an elliptic PDE. In contrast, we employ kernel models and determine their coefficients by solving the optimization problem.

The equivalence to the weak formulation allows for rigorous error analysis using standard techniques from numerical analysis. We thus obtain a priori convergence estimates for the proposed method. Such a priori error estimates are hard to derive for neural networks since the set of neural networks does not form a linear space and therefore results such as Céa’s Lemma are not applicable in that case. For kernel methods we prove convergence results with respect to the  $H^1$ -norm and the  $L^2$ -norm in this contribution. These results show that the convergence rate of the approximation in terms of the mesh norm depends on the smoothness of the weak solution and on the regularity of the kernel. It is therefore possible to obtain smaller errors by reducing the mesh norm, whereas for neural networks it is typically unclear what part of the neural network architecture to adjust, i.e. whether to increase the number of layers or the number of neurons or whether to choose a different activation function. Additionally, the solution can even be improved locally in space by adding more centers in certain parts of the domain – and we aim to follow up with this, e.g. by leveraging greedy kernel methods [36]. Certainly, kernel methods involve several hyperparameters as well, such as the shape parameter, but the convergence results are independent of these parameters and are asymptotically only influenced by the smoothness of the kernel.

We examined the performance of kernel methods within the deep Ritz approach by means of two numerical examples. In the first experiment we considered a PDE with a smooth solution such that the convergence rate is limited by the smoothness of the kernel according to Theorems 4 and 5. The second experiment is based on a non-convex domain with a re-entrant corner that leads to a singular solution with low regularity. As expected, the numerical experiment shows that the convergence rate is independent of the smoothness of the kernel and instead determined by the regularity of the solution.

Meshless methods such as the kernel approaches based on the deep Ritz ansatz as described in this paper circumvent the necessity of computing a computational mesh. Furthermore, the algorithms described in this contribution can be implemented with relatively small effort. A (local) refinement of the solution is also readily possible by adding more centers. Finite element methods in contrast would require a mesh refinement or a higher order approach to improve the solution.

Future research extending on the results obtained in this paper might for instance be concerned with the application of other kernel approaches, such as deep kernel methods, see [35, 37], within the deep Ritz approach. These deep kernel methods allow for a multi-layer structure to improve the approximation properties of the resulting functions. It might be of interest to investigate the performance of deep kernel methods when applied to the examples given in this paper. Furthermore, one could examine the

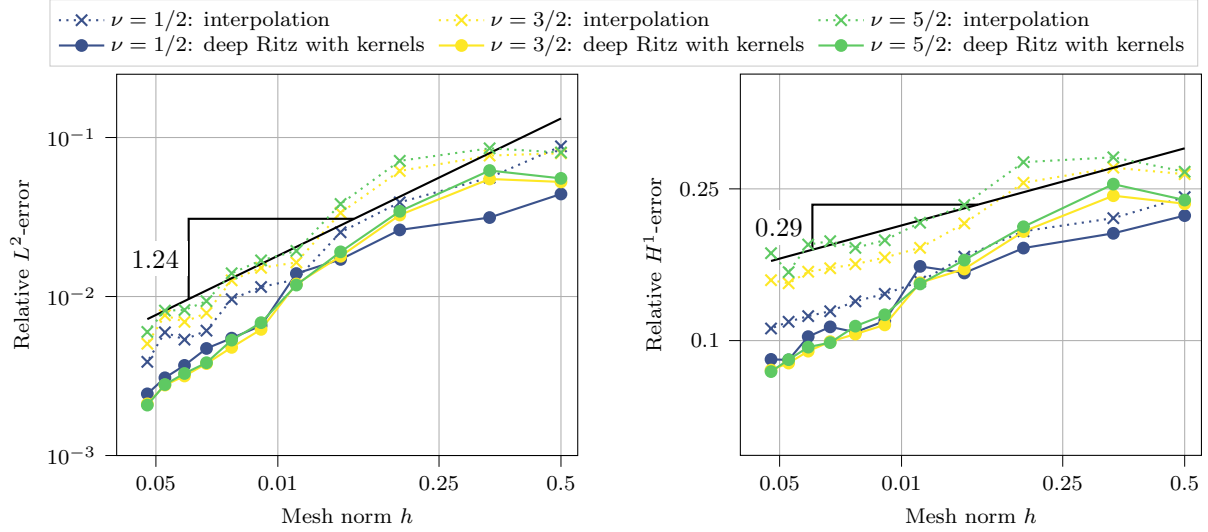


Figure 5: Relative errors in the  $L^2$ -norm (left) and the  $H^1$ -norm (right) with respect to the mesh norm  $h$  for Matérn kernels of smoothness  $\nu \in \{1/2, 3/2, 5/2\}$  in the example with a singular solution. The dashed lines indicate the error decays of the interpolation of the exact solution by the respective kernel. The estimated convergence rate for the interpolation with  $\nu = 5/2$  is shown as a black line.

approach in higher spatial dimensions and compare the results to those obtained by neural networks. We expect that certain deep kernel approaches achieve at least similar results as neural networks also in high dimensions if the actual weak solution possesses an inherently low-dimensional structure. In order to further improve the performance of the kernel methods when adding more centers, compactly supported kernels such as the class of Wendland kernels might be useful. It would moreover be of interest to derive an a posteriori error estimate that can be evaluated efficiently.

## References

- [1] Atılım Günes Baydin, Barak A. Pearlmutter, Alexey Andreyevich Radul, and Jeffrey Mark Siskind. “Automatic differentiation in machine learning: a survey”. In: *Journal of Machine Learning Research* 18.1 (2017), pp. 5595–5637.
- [2] T. Belytschko, Y. Krongauz, D. Organ, M. Fleming, and P. Krysl. “Meshless methods: An overview and recent developments”. In: *Computer Methods in Applied Mechanics and Engineering* 139.1–4 (1996), pp. 3–47. DOI: 10.1016/s0045-7825(96)01078-x.
- [3] Joseph Benzaken, John A. Evans, and Rasmus Tamstorf. “Constructing Nitsche’s Method for Variational Problems”. In: *Archives of Computational Methods in Engineering* 31.4 (2024), pp. 1867–1896. DOI: 10.1007/s11831-023-09953-6.
- [4] Steven L. Brunton and J. Nathan Kutz. “Promising directions of machine learning for partial differential equations”. In: *Nature Computational Science* 4.7 (2024), pp. 483–494. DOI: 10.1038/s43588-024-00643-2.
- [5] Philippe G. Ciarlet. *The Finite Element Method for Elliptic Problems*. Society for Industrial and Applied Mathematics, 2002. DOI: 10.1137/1.9780898719208.
- [6] Jean C ea. “Approximation variationnelle des probl emes aux limites”. In: *Annales de l’institut Fourier* 14.2 (1964), pp. 345–444. DOI: 10.5802/aif.181.
- [7] Yong Duan. “A note on the meshless method using radial basis functions”. In: *Computers & Mathematics with Applications* 55.1 (2008), pp. 66–75. DOI: 10.1016/j.camwa.2007.03.011.
- [8] Weinan E and Bing Yu. “The Deep Ritz Method: A Deep Learning-Based Numerical Algorithm for Solving Variational Problems”. In: *Communications in Mathematics and Statistics* 6.1 (2018), pp. 1–12. DOI: 10.1007/s40304-018-0127-z.



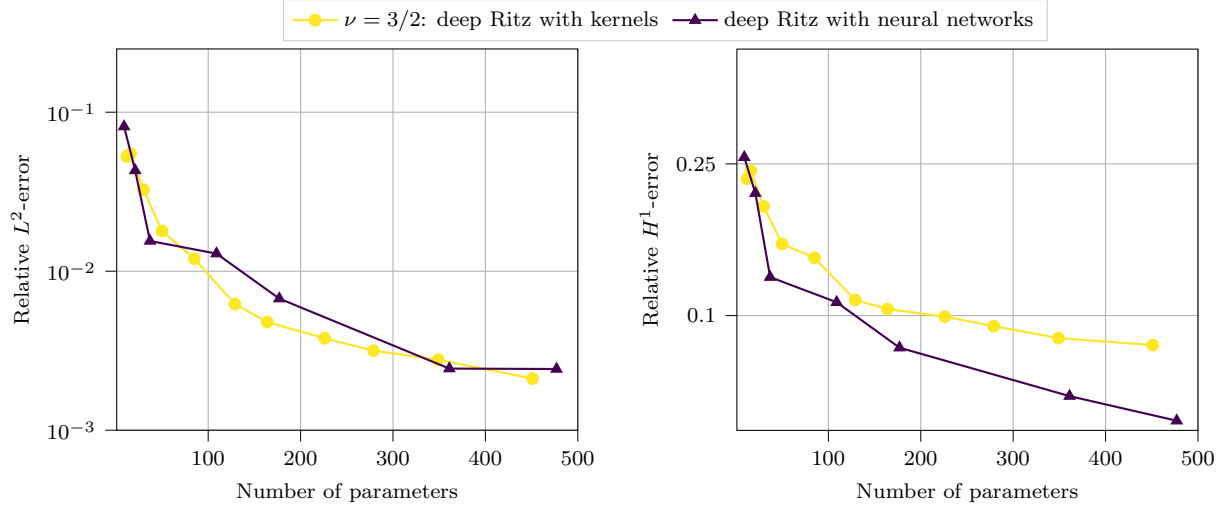


Figure 6: Relative errors in the  $L^2$ -norm (left) and the  $H^1$ -norm (right) with respect to the number of parameters for Matérn kernels of smoothness  $\nu = 3/2$  and fully-connected neural networks in the example with a singular solution.

- [9] Lawrence Evans. *Partial Differential Equations*. American Mathematical Society, 2010. DOI: 10.1090/gsm/019.
- [10] Bengt Fornberg and Natasha Flyer. *A Primer on Radial Basis Functions with Applications to the Geosciences*. Society for Industrial and Applied Mathematics, 2015. DOI: 10.1137/1.9781611974041.
- [11] Carsten Franke and Robert Schaback. “Solving partial differential equations by collocation using radial basis functions”. In: *Applied Mathematics and Computation* 93.1 (1998), pp. 73–82.
- [12] Yuling Jiao, Yanming Lai, Yisu Lo, Yang Wang, and Yunfei Yang. “Error analysis of deep Ritz methods for elliptic equations”. In: *Analysis and Applications* 22.01 (2023), pp. 57–87. DOI: 10.1142/s021953052350015x.
- [13] E.J. Kansa. “Multiquadrics — A scattered data approximation scheme with applications to computational fluid-dynamics. I. Surface approximations and partial derivative estimates”. In: *Computers & Mathematics with Applications* 19.8 (1990), pp. 127–145. DOI: 10.1016/0898-1221(90)90270-T.
- [14] George S. Kimeldorf and Grace Wahba. “A Correspondence Between Bayesian Estimation on Stochastic Processes and Smoothing by Splines”. In: *The Annals of Mathematical Statistics* 41.2 (1970), pp. 495–502. DOI: 10.1214/aoms/1177697089.
- [15] Diederik P. Kingma and Jimmy Ba. *Adam: A Method for Stochastic Optimization*. 2014. DOI: 10.48550/ARXIV.1412.6980.
- [16] Hendrik Kleikamp and Tizian Wenzel. *Software for “Kernel Methods in the Deep Ritz framework: Theory and practice”*. 2024. DOI: 10.5281/zenodo.13890995. URL: <https://zenodo.org/records/13890995>.
- [17] Jens Künemund, Francis J. Narcowich, Joseph D. Ward, and Holger Wendland. “A high-order meshless Galerkin method for semilinear parabolic equations on spheres”. In: *Numerische Mathematik* 142.2 (2019), pp. 383–419. DOI: 10.1007/s00211-018-01021-7.
- [18] Yulong Lu, Jianfeng Lu, and Min Wang. “A Priori Generalization Analysis of the Deep Ritz Method for Solving High Dimensional Elliptic Partial Differential Equations”. In: *Proceedings of Thirty Fourth Conference on Learning Theory*. Ed. by Mikhail Belkin and Samory Kpotufe. Vol. 134. Proceedings of Machine Learning Research. PMLR, 2021, pp. 3196–3241.
- [19] Pingbing Ming and Yulei Liao. “Deep Nitsche Method: Deep Ritz Method with Essential Boundary Conditions”. In: *Communications in Computational Physics* 29.5 (2021), pp. 1365–1384. DOI: 10.4208/cicp.oa-2020-0219.

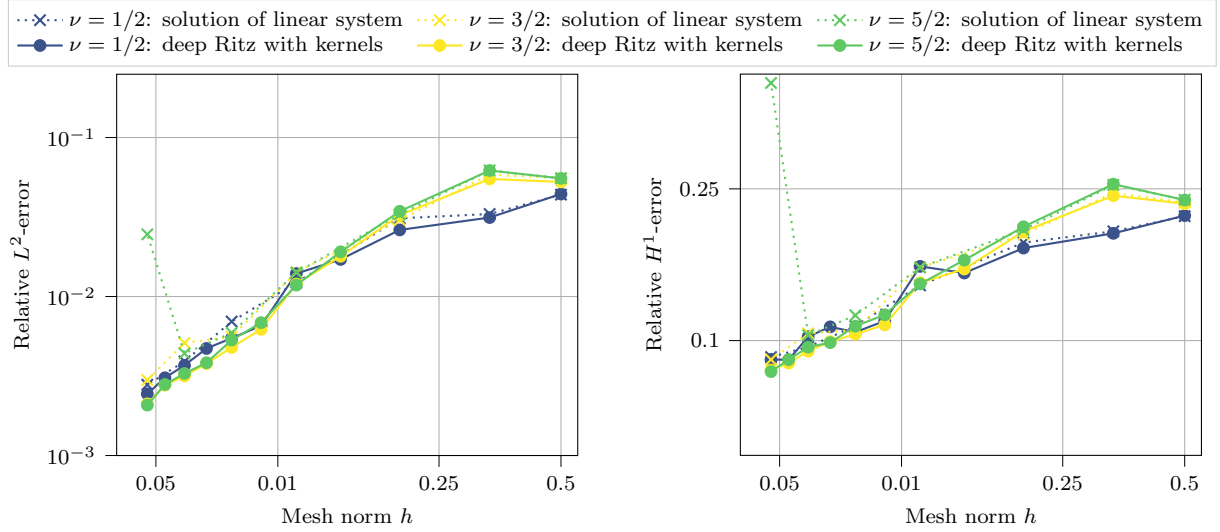


Figure 7: Relative errors in the  $L^2$ -norm (left) and the  $H^1$ -norm (right) with respect to the mesh norm  $h$  for Matérn kernels of smoothness  $\nu \in \{1/2, 3/2, 5/2\}$  using the energy minimization problem and the linear system of equations in the example with a singular solution.

- [20] Johannes Müller and Marius Zeinhofer. *Deep Ritz revisited*. 2019. DOI: 10.48550/ARXIV.1912.03937.
- [21] Francis Narcowich, Joseph Ward, and Holger Wendland. “Sobolev bounds on functions with scattered zeros, with applications to radial basis function surface fitting”. In: *Mathematics of Computation* 74.250 (2004), pp. 743–763. DOI: 10.1090/s0025-5718-04-01708-9.
- [22] Francis Narcowich, Joseph Ward, and Holger Wendland. “Sobolev Error Estimates and a Bernstein Inequality for Scattered Data Interpolation via Radial Basis Functions”. In: *Constructive Approximation* 24.2 (2006), pp. 175–186. DOI: 10.1007/s00365-005-0624-7.
- [23] Francis J. Narcowich, Stephen T. Rowe, and Joseph D. Ward. “A novel Galerkin method for solving PDEs on the sphere using highly localized kernel bases”. In: *Mathematics of Computation* 86.303 (2016), pp. 197–231. DOI: 10.1090/mcom/3097.
- [24] J. Nitsche. “Über ein Variationsprinzip zur Lösung von Dirichlet-Problemen bei Verwendung von Teilräumen, die keinen Randbedingungen unterworfen sind”. In: *Abhandlungen aus dem Mathematischen Seminar der Universität Hamburg* 36.1 (1971), pp. 9–15. DOI: 10.1007/bf02995904.
- [25] Adam Paszke, Sam Gross, Francisco Massa, Adam Lerer, James Bradbury, Gregory Chanan, Trevor Killeen, Zeming Lin, Natalia Gimelshein, Luca Antiga, Alban Desmaison, Andreas Köpf, Edward Yang, Zach DeVito, Martin Raison, Alykhan Tejani, Sasank Chilamkurthy, Benoit Steiner, Lu Fang, Junjie Bai, and Soumith Chintala. “PyTorch: an imperative style, high-performance deep learning library”. In: *Proceedings of the 33rd International Conference on Neural Information Processing Systems*. Red Hook, NY, USA: Curran Associates Inc., 2019.
- [26] Vivek G. Patel and Nikunj V. Rachchh. “Meshless method – Review on recent developments”. In: *Materials Today: Proceedings* 26 (2020), pp. 1598–1603. DOI: 10.1016/j.matpr.2020.02.328.
- [27] M. Raissi, P. Perdikaris, and G.E. Karniadakis. “Physics-informed neural networks: A deep learning framework for solving forward and inverse problems involving nonlinear partial differential equations”. In: *Journal of Computational Physics* 378 (2019), pp. 686–707. DOI: 10.1016/j.jcp.2018.10.045.
- [28] Robert Schaback. “Superconvergence of kernel-based interpolation”. In: *Journal of Approximation Theory* 235 (2018), pp. 1–19. DOI: 10.1016/j.jat.2018.05.002.
- [29] Gilbert Strang. “Variational crimes in the finite element method”. In: *The Mathematical Foundations of the Finite Element Method with Applications to Partial Differential Equations*. Elsevier, 1972, pp. 689–710. DOI: 10.1016/b978-0-12-068650-6.50030-7.

- [30] Zhengjie Sun and Leevan Ling. “A Kernel-Based Meshless Conservative Galerkin Method for Solving Hamiltonian Wave Equations”. In: *SIAM Journal on Scientific Computing* 44.4 (2022), A2789–A2807. DOI: 10.1137/21m1436981.
- [31] Yuki Ueda and Norikazu Saito. “The inf-sup condition and error estimates of the Nitsche method for evolutionary diffusion–advection–reaction equations”. In: *Japan Journal of Industrial and Applied Mathematics* 36.1 (2018), pp. 209–238. DOI: 10.1007/s13160-018-0338-4.
- [32] Carlos Uriarte, David Pardo, Ignacio Muga, and Judit Muñoz-Matute. “A Deep Double Ritz Method (D<sup>2</sup>RM) for solving Partial Differential Equations using Neural Networks”. In: *Computer Methods in Applied Mechanics and Engineering* 405 (2023), p. 115892. DOI: 10.1016/j.cma.2023.115892.
- [33] Holger Wendland. “Meshless Galerkin methods using radial basis functions”. In: *Mathematics of Computation* 68.228 (1999), pp. 1521–1531. DOI: 10.1090/s0025-5718-99-01102-3.
- [34] Holger Wendland. *Scattered Data Approximation*. Cambridge University Press, 2004. DOI: 10.1017/cbo9780511617539.
- [35] Tizian Wenzel, Francesco Marchetti, and Emma Perracchione. “Data-Driven Kernel Designs for Optimized Greedy Schemes: A Machine Learning Perspective”. In: *SIAM Journal on Scientific Computing* 46.1 (2024), pp. C101–C126. DOI: 10.1137/23m1551201.
- [36] Tizian Wenzel, Gabriele Santin, and Bernard Haasdonk. “Analysis of target data-dependent greedy kernel algorithms: Convergence rates for  $f$ -,  $f \cdot P$ - and  $f/P$ -greedy”. In: *Constructive Approximation* 57.1 (2023), pp. 45–74. DOI: doi.org/10.1007/s00365-022-09592-3.
- [37] Tizian Wenzel, Gabriele Santin, and Bernard Haasdonk. *Universality and Optimality of Structured Deep Kernel Networks*. 2021. DOI: 10.48550/ARXIV.2105.07228.

## Statements and declarations

### Funding

- H. Kleikamp acknowledges funding by the Deutsche Forschungsgemeinschaft (DFG, German Research Foundation) under Germany’s Excellence Strategy EXC 2044 –390685587, Mathematics Münster: Dynamics–Geometry–Structure.
- T. Wenzel acknowledges financial support through the projects LD-SODA of the *Landesforschungsförderung Hamburg* (LFF) and support from the RTG 2583 “Modeling, Simulation and Optimization of Fluid Dynamic Applications” funded by the *Deutsche Forschungsgemeinschaft* (DFG).

**Competing interests** The authors have no relevant financial or non-financial interests to disclose.

**Code availability** The source code used to carry out the numerical experiments presented in this contribution can be found in [16].